http://dx.doi.org/10.5935/0103-5053.20140107

J. Braz. Chem. Soc., Vol. 25, No. 7, 1275-1282, 2014.
Printed in Brazil - ©2014 Sociedade Brasileira de Química
0103 - 5053 $6.00+0.00

Article

Side-Chain Liquid-Crystalline Polymer Tetrazoles: Synthesis and Characterization

Muhammad Tariq,[a,b] Shahid Hameed,[b] Rachel F. Magnago,[c] Ivan H. Bechtold[d] and Aloir A. Merlo*[a]*

[a]*Instituto de Química, Universidade Federal do Rio Grande do Sul (UFRGS), Av. Bento Gonçalves, 9500, Bairro Agronomia, 91501-970 Porto Alegre-RS, Brazil*

[b]*Department of Chemistry, Quaid-i-Azam University, 45320 Islamabad, Pakistan*

[c]*Unidade Tecnológica, Universidade do Sul de Santa Catarina (Unisul), Av. Pedra Branca, 25, Cidade Universitária, 88137-270 Palhoça-SC, Brazil*

[d]*Departamento de Física, Universidade Federal de Santa Catarina (UFSC), Bairro Trindade, 88040-900 Florianópolis-SC, Brazil*

A síntese e o comportamento de fase de três novos polímeros cristais líquidos de cadeia lateral são descritos. Os novos polímeros apresentaram mesofase esmética C (SmC). O estudo de raios X para duas amostras revelou parcial interdigitação para a mesofase SmC do polímero com espaçador mais curto, enquanto que com espaçador mais longo o polímero não apresentou interdigitação.

The synthesis and phase behavior of three new side-chain liquid crystal polymers with short and long flexible alkyl spacers are described. These new materials show smectic C (SmC) mesophase. X-ray analysis for two samples has revealed that SmC mesophase displays partial interdigitation for the polymer with short flexible spacer, while for long flexible spacer polymer no interdigitation was observed.

Keywords: tetrazoles, homopolymer liquid crystals, polyacrylates and SmC mesophase

Introduction

The synthesis and studies of the physical properties of thermotropic liquid crystals are the subjects of current interest as thermotropic liquid crystals have technological applications in electro-optic devices.[1,2] From the viewpoint of the science basics, this interest is evident by numerous studies of both low- and high-molecular weight liquid crystals[3-9] indicating the structural dependence of liquid-crystalline properties. However, the relationship between structural aspects and mesophase behavior is not well understood.

Liquid crystals (LCs) are systems that can self-organize due to mesogenic groups that exhibit cooperative interactions among them. This is the origin of interesting properties of liquid crystals and extends to both types of high-molecular weight liquid crystals, i.e., side- and main-chain liquid crystalline polymers (SCLCP and MCLCP, respectively). It is well known that the nature of mesophases depends on the relationship established between polymer backbone, mesogenic core and the length of the flexible spacer group. Some studies regarding tetrazole derivatives with LC behavior have recently been reported in the literature.[10-12]

In order to investigate the correlation between flexible spacer length, molecular weight and the influence of tetrazole ring we have synthesized three polymer LCs containing *N*-alkylated tetrazole ring as part of mesogenic core connected to the polyacrylate backbone through flexible spacer with four and eleven carbon atoms. The tetrazole ring was built by 1,3-dipolar addition of azide anion (N_3^-) to an arylnitrile and regioselectively alkylation at position 2. The regioselectivity during the alkylation step has been recently established unequivocally by single crystal X-ray analysis for two final LCs.[13]

Results and Discussion

Synthesis

The preparation of key intermediate **3** is outlined in Scheme 1. It was prepared in four steps starting from cyanophenol **1** using protection-deprotection strategy to

*e-mail: shameed@qau.edu.pk, aloir.merlo@ufrgs.br

prevent *O*-alkylation reaction. The tetrazole heterocycle was constructed by [3+2] 1,3-dipolar cycloaddition of azide anion to cyanophenol **1** followed by acetylation of phenol functionality to yield **2** in 51% yield over two steps. The alkylation of **2** with nonylbromide yielded the corresponding *N*-2 nonyl tetrazolylacetate, which was subsequently hydrolyzed in basic solution to furnish the free phenol **3** in 87% yield.

The synthesis of acids **6** and **8** carrying the polymerizable acrylate group is outlined in Scheme 2 and 3, respectively. The acrylate group was introduced using a large excess of acrylic acid in presence of *p*-toluene sulfonic acid (*p*TSA) and hydroquinone.[14] The former was prepared according to a method described by Portugal *et al.*.[15] The only modification made in this method was in the first step, when 4-chlorobutyl acetate was employed instead of 4-bromobutyl acetate. 4-Chlorobutyl acetate was obtained from ring opening reaction of tetrahydrofuran (THF) with acetylchloride and catalytic amount of zinc chloride as outlined in Scheme 2.

The intermediate **8**[14] was prepared in three steps as depicted in Scheme 3. The flexible spacer has eleven methylene carbon atoms and the polymerizable acrylate group was introduced in the same way as described for compound **6**. The target acrylates **6** and **8** were isolated and purified by recrystallization from isopropanol or aqueous ethanol.

Monomers **9** and **10** were prepared from 4-[(4-propenoyloxy)butyloxy]benzoic acid **6** and 4-[(4-propenoyloxy)undecyloxy]benzoic acid **8**, respectively, by reacting with tetrazolylphenol **3** using dicyclohexyl carbodiimide (DCC) in pyridine solution and *p*TSA as a catalyst.[15] The yields after purification were in range of 30-60%. The monomers were subjected to free radical polymerization in toluene using 2,2'-azobisisobutyronitrile (AIBN) as radical initiator to give homopolymers **11** and **12** (Scheme 4). The polymers were purified by successive precipitation with a solution of dichloromethane in cold methanol. Finally, the amorphous solid was washed several times with cold ethyl acetate until

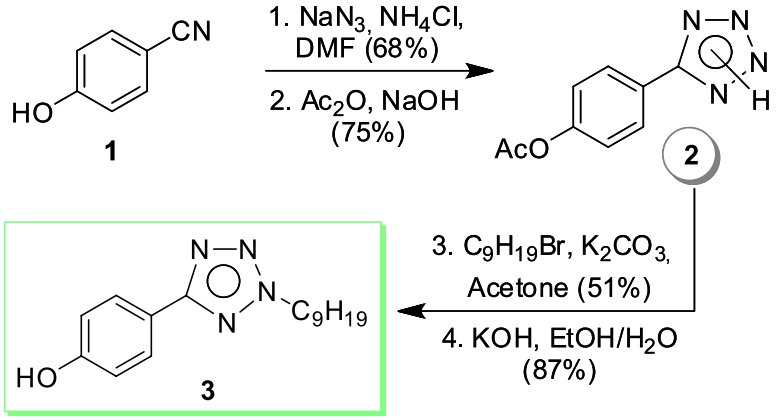

Scheme 1. Synthesis of *N*-2 nonyltetrazolylphenol **3**.

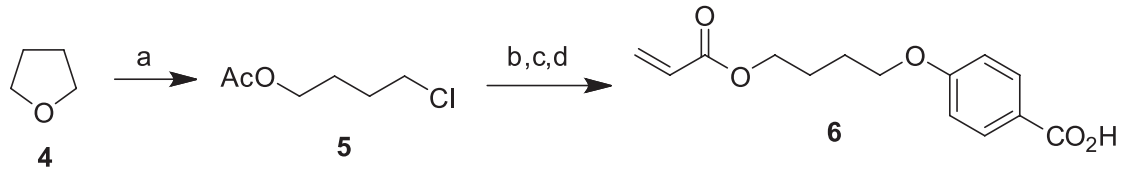

Scheme 2. Reaction conditions: (a) AcOCl, $ZnCl_2$ (cat); (b) KOH, *p*-$HOPhCO_2Me$, *N,N*-dimethyl formamide (DMF)/benzene (85%); (c) (*i*) KOH, ethanol/water; (*ii*) HCl, H_2O (90%); (d) CH_2=$CHCO_2H$, *p*TSA, hydroquinone, $CHCl_3$ (75%).

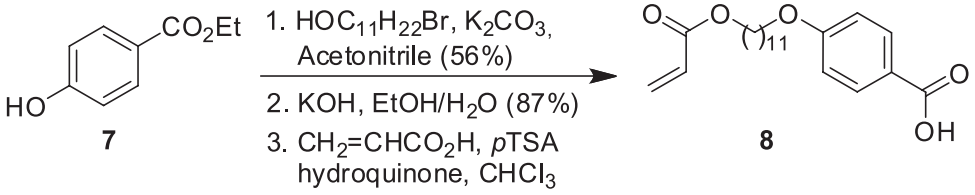

Scheme 3. Synthesis of polymerizable acrylate **8**.

no signal for ethylenic protons was observed in nuclear magnetic resonance (NMR) analysis. The comparative data of the homopolymers **11a**,**b** and **12** are shown in Table 1.

Liquid-crystalline properties

The mesomorphic properties of the polymers were studied using polarizing optical microscopy (POM) and differential scanning calorimetry (DSC). The texture of the mesophase[16] was identified by microscopic studies on cooling from the isotropic to mesomorphic state. The liquid-crystalline properties of the polymers **11a**,**b** and **12** are compiled in Table 1. Table 1 lists the observed layer spacing obtained from the Bragg equation and the calculated length of the monomer molecule obtained from the program ChemBio3D Ultra.

The synthesis of polyacrylate **11a** was carried out using 3 wt.% of AIBN while polymerization reaction to give **11b** and **12** were performed using 5 wt.% of AIBN. The molecular weight (Mn) and degree of polymerization (DP) for **11a** is twice than **11b** and **12**, probably related to the content of initiator during the chemical polymerization process. Polymers **11b** and **12** may be considered as oligomers considering the low value of DP for these polymers. All the polymers exhibited a glass transition temperature (Tg) and enantiotropic SmC phase. For instance, polymer **12** shows Tg at 70.5 °C and enters the smectic C phase with a range of 36.5 °C for the mesophase and goes to isotropic phase at 107 °C. The flexible spacers in this study have four and eleven methylene carbon atoms. The polymer backbone for **11a** and **11b** are closer to the mesogenic core while in **12** it is relatively away from the mesogenic core. However, the mesomorphic behavior does not drastically change with lengthening of the flexible spacer. Even the variation of the DP was not enough to change the nature of the mesophase or to significantly alter the mesophase range as is evident form the comparison of DP for **11a** and **11b**, where the first is almost twice as heavier as the second. Previously reported results have revealed that when the mesogenic core is derived from 1,4-phenylene unit, the mesophase is nematic in the case of a short flexible spacer and smectic A phase for long flexible spacer.[17] Considering the polymeric nature of **11a**,**b** and **12** and that they do not tend to crystallize on cooling a mesophase fixation when the samples were exposed to polymerization action. From POM analysis, both polymers show a glassy appearance. The glass transition temperature tends to decrease as the molecular weight decreases for polymers with the same flexible spacer, compare **11a** and **11b**. The Tg tends to be higher for a polymer that has longer flexible spacer as observed for **12**. In general, a lower polymer glass transition temperature implies that the backbone is more flexible.

Data compiled in Table 1 shows that the shortening or lengthening of flexible spacer does not have any influence on the nature of the mesophase. However, as will be discussed in the X-ray section, the structure of SmC phase is dependent on the length of flexible spacer. Smectic C phase observed

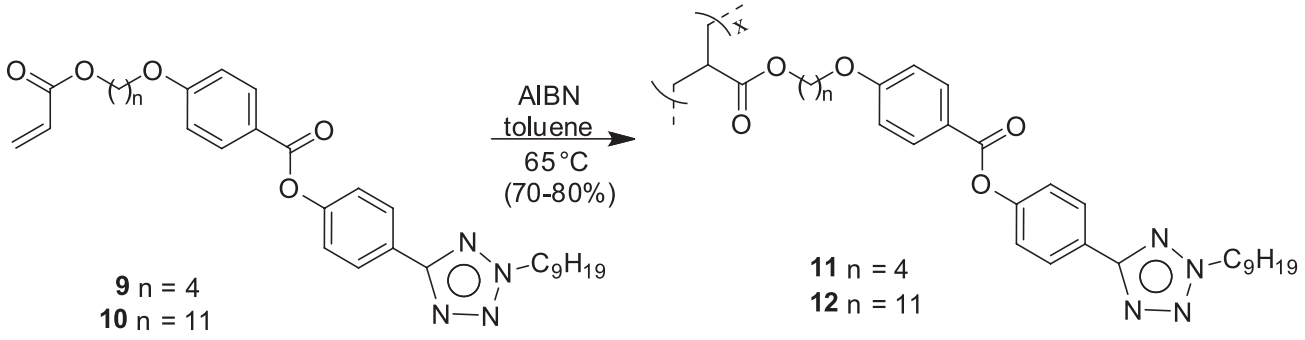

Scheme 4. Synthesis of polymers **11** and **12**.

Table 1. Data for polymers **11a**,**b** and **12**: GPC, transition temperature and X-ray diffraction

entry	Mn	Mw/Mn	DP	Yield / %	Transition temperatures[a] / °C	Observed layer spacing (*l*) / Å[b]	Calc. layer spacing (*d*) / Å[c]
11a	7460	1.2	14	69	g 70 SmC 129 I	–	–
11b	4420	1.2	8	85	g 54 SmC 130 I	45.2:23.8:16.1	32.8
12	4520	1.3	7	78	g 71 SmC 107 I	36.6	40.4

[a]Transition temperatures were acquired upon heating by POM; [b]data collected at 90 °C; [c]data collected at 80 °C. Mn: g mol^{-1}; DP: number average degrees of polymerization; GPC: gel permeation chromatography.

in this study probably is the result of folded-shape of the mesogenic core having a non-symmetrical tetrazole ring. The folded-shape of mesogenic core prints on the polymer material its structural feature, which overcomes the tendency of the main-chain to adopt a random coil conformation.[18]

The mesomorphic behavior of compounds **11a**,**b** and **12** was investigated between crossed polarizers using optical microscopy. Figure 1a displays the normal texture for **11a**,**b** and **12.** Schieliren texture is barely seen in this picture due to the nature of the sample and the thickness. However, in other areas where the thickness is smaller, especially in the border zone of the samples, the Schlieren texture flourishes radiantly (Figure 1b). The Schlieren texture with four-point brushes characteristic of smectic C phase is seen for **11b** (Figure 1b). The assignment to nematic phase was discarded considering that from isotropic phase no droplets were observed upon cooling. Also, the absence of optically extinct homeotropic and flashing areas on the mechanical disturbance corroborates to eliminate the nematic phase.

X-Ray diffraction studies

X-Ray diffraction (XRD) studies were carried out to confirm the POM results and obtain more detailed information on the structures and types of liquid crystalline phases. Generally, a diffuse broad peak where 2θ assumes values from 16 to 22° in the wide angle region of X-ray diffraction curves can be observed for polymers but not for polymer LCs with smectic, nematic, and N* phase structures due to the average distance between the mesogenic groups. Sharp and strong peaks at low angles in which 2θ assumes values from 1 to 5° can be observed for a normal smectic structure which exhibits a layered packing arrangement, but not for N* and nematic structures.

Figure 2 shows the patterns of compounds **11b** and **12** to investigate the structure of their smectic phases at 90 and 80 °C, respectively. In both cases the spectrum contains a sharp peak in the low-angle region corresponding to the Miller index (001), where by applying Bragg's law resulted in an interlayer spacing of 45.2 ± 0.1 Å for **11b** and 36.6 ± 0.1 Å for **12**. In addition, a broad diffuse band centered around 4.4 Å is present, which is related to the short-range correlations between neighboring mesogenic molecules inside the layers. Compound **11b** also displayed secondary order peaks (002) and (003) corresponding to distances of 23.8 ± 0.1 and 16.1 ± 0.1 Å, respectively, following the relation 1:2:3 with respect to (001), as expected for smectic phases. However, only the (001) is observed for compound **12**, which indicates that the smectic order is short range correlated. The molecular length of the monomer molecules **9** and **10** was calculated with the program ChemBio3D Ultra considering the most extended configuration, giving 32.8 ± 0.1 and 40.4 ± 0.1 Å, respectively. One can see that the calculated value for monomer **10** is around 3.8 Å larger than the interlayer distance measured for polymer **12**, which is consistent with conformational disorder of the aliphatic chains and inclination of the molecules inside the layers expected for the SmC phase. On the other hand, monomer **9** is around 12.4 Å shorter than the interlayer distance measured for polymer **11b**. The ratio between the interlayer distance and the molecular length is 1.38 and this observation is consistent with a partial interdigitation of the mesogens inside the layers.

If we consider that the backbone is confined by the smectic field and lies between the layers,[19] two arrangements for polymers **11b** and **12** are possible. In one arrangement, the side chains are closer to the backbone than in the other, causing a partially interdigitated SmC phase. In the other arrangement, the side chains exhibit no interdigitation. In both cases, the motion of the backbone is constrained by the orientational and positional order of the smectic layer.

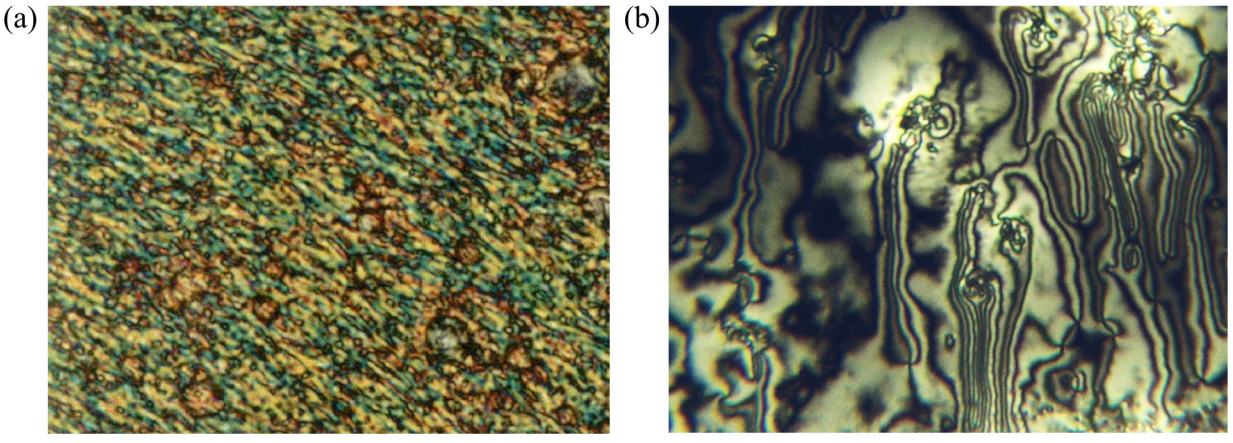

Figure 1. Schlieren texture observed for polymer **11a** at room temperature (a) and **11b** at 10 °C (b).

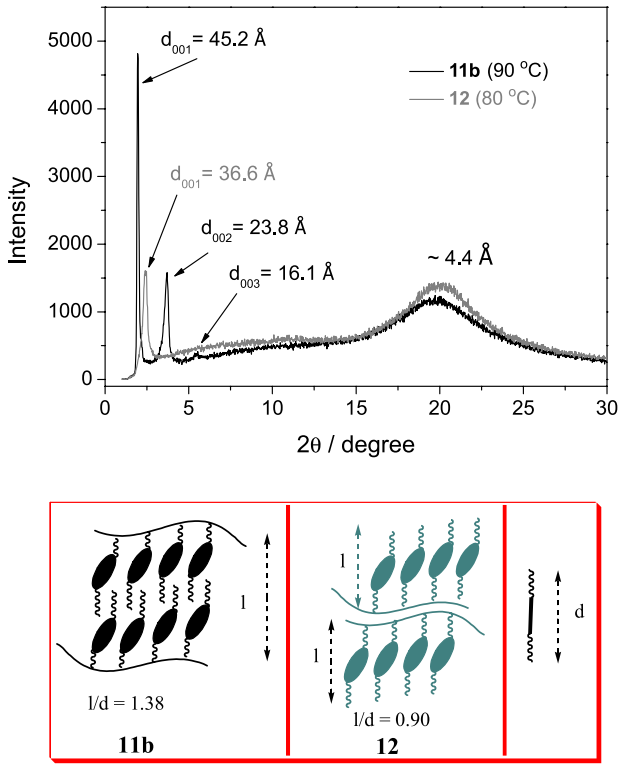

Figure 2. (Top) X-Ray diffraction patterns for compound **11b** (black line) and **12** (gray line), with indication of the Miller indices. SmC phase at 90 and 80 ºC for **11b** and **12**, respectively. (Bottom) Two types of smectic C structure exhibited by side-chain liquid crystal polymers **11b** and **12**.

The evidence for this classification comes from other data published in the literature.[20] From Table 1, the higher glass transition temperature is observed for **12,** which exhibits no interdigitated smectic phase. The side chains are more decoupled from the polymer backbone due to the longer flexible spacer. The anisotropic cores have more freedom to arrange themselves in an appropriate manner with more independence from the main chain orientation of backbone. For polymer **11b**, with smaller flexible spacer, the behavior is similar to the nematic one. In this sense, it is possible to expect some interdigitation of the laterally anisotropic core. These structural features of the smectic phase have pronounced effects on packing density as well as transition properties. Mesophase structure that possesses a more compactness degree has a less specific free volume.[21] The closer the mesogenic cores to the random coil conformation of polymer, the higher the influence of polymer backbone on the final structure of the mesophase. The main chain was no longer a random coil. A considerable degree of mesogenic order is transferred to the main chain by the flexible spacer.[18,22] The behavior of **11b** is in accordance with the general tendency that the increasing backbone flexibility for a given spacer length and mesogenic core tends to diminish the glass transition temperature while increasing the temperature of clearing (Tc) or the clearing point.[2,15,23]

Conclusions

In summary, we have synthesized three homopolymers having the tetrazole ring as the key structural brick for the mesomorphic phenomenon. They showed smectic C enantiotropic behavior with a large mesophase range. Flexibility of polymer backbone, Tg and Tc transition temperatures are dependent on the polymerization degree. These are important parameters to be considered in the design and synthesis of new materials. X-Ray analysis showed a partial interdigitation of the mesogens inside the layers of the polymer with short flexible spacer.

Experimental

Characterization

^{1}H and ^{13}C NMR spectra were recorded on a Bruker AC-300F spectrometer in $CDCl_3$, using tetramethylsilane (TMS) as the internal standard. Infrared (IR) spectra were recorded on a Perkin-Elmer 781 spectrometer in KBr disc or film. The thermal transitions and the mesomorphic textures of the compounds were observed by optical microscopy using a Leitz Ortholux polarizing microscope in conjunction with a Mettler FP 52 heating stage. The XRD experiments were carried out using X'PERT-PRO (PANalytical) diffractometer using the linear monochromatic Cu Kα radiation (λ = 1.5418 Å) and applied power of 1.2 kVA. The samples consisted of an amount of powder on a glass plate placed in the diffractometer chamber on the TCU2000 temperature control unit (Anton Paar), allowing temperature control during the measurement. The scans were performed in continuous mode from 2 to 30° (2θ angle) with the samples in the mesophase, obtained by cooling from the isotropic state.

Synthesis

All reagents were purchased from Aldrich Chemical Company (USA) and solvents were used as received from Merck. The synthesis of the title compounds were carried out according to standard methods outlined in Schemes 1, 2, 3 and 4.

4-(2*H*-Tetrazol-5-yl)phenyl acetate (**2**)

(*i*) 4-(2*H*-Tetrazol-5-yl)phenol: To a solution of 4-cyanophenol (**1**) (5.0 g, 0.042 mol) in 28 mL *N,N*-dimethyl formamide (DMF) was added sodium azide (11.0 g, 0.17 mol) and ammonium chloride (9.0 g, 0.17 mol). The mixture was stirred for 24 h maintaining the temperature at 120 °C. The reaction mixture was

cooled to room temperature and was poured into 50 mL of ice cold water. The mixture was acidified with concentrated HCl to pH 2. The precipitate formed was filtered off and the product was recrystallized from ethanol giving orange crystals. Yield 68%; m.p. 241.8 °C; R_f = 0.23 (*n*-hexane:ethyl acetate; 6:4); IR (KBr) ν_{max}/cm^{-1} 3445, 3254, 2930, 2845, 1608; ^{1}H NMR ($CDCl_3$, 300 MHz) δ 4.65 (s broad, 1H, NH); 7.3 (d, 2H, *J* 6.6 Hz, Ar–H); 8.1 (d, 2H, *J* 6.6 Hz, Ar–H); 10.3 (s broad, 1H, OH); ^{13}C NMR ($CDCl_3$, 75 MHz) δ 122.6, 125.5, 127.3, 152.2, 169.4.

(*ii*) 4-(2*H*-Tetrazol-5-yl)phenyl acetate (**2**): To a 3 mol L^{-1} sodium hydroxide solution (27.6 mL) was added 4-(2*H*-tetrazol-5-yl)phenol (5.4 g, 0.03 mol). The mixture was cooled in an ice bath followed by dropwise addition of acetic anhydride (7.9 mL, 0.084 mol) along with some ice. The reaction mixture was vigorously stirred for 30 min and the precipitate formed was filtered off, washed with cold water and recrystallized from water-methanol. Yield 58%; white solid; m.p. 182 °C; R_f = 0.33 (*n*-hexane:ethyl acetate; 6:4); IR (KBr) ν_{max}/cm^{-1} 3075, 2938, 2844, 1758, 1613, 1200; ^{1}H NMR ($CDCl_3$, 300 MHz) δ 2.3 (s, 3H, CH_3), 6.2 (s, broad, 1H, NH), 7.4 (d, 2H, *J* 6.6 Hz, Ar–H), 8.1 (d, 2H, *J* 6.6 Hz, Ar–H); ^{13}C NMR ($CDCl_3$, 75 MHz) δ 22.9, 122.4, 125.2, 128.0, 153.0, 158.0, 169.0.

4-(2-Nonyl-2*H*-tetrazol-5-yl)phenol (**3**)

(*i*) 4-(2-Nonyl-2*H*-tetrazol-5-yl)phenyl acetate: A mixture of 4-(2*H*-tetrazol-5-yl)phenyl acetate (**2**) (2.50 g, 0.012 mol), nonylchloride (1.95 g, 0.012 mol) and anhydrous potassium carbonate (1.65 g, 0.012 mol) in 30 mL acetone was heated under reflux for 48 h. The reaction mixture was cooled to room temperature and filtered. The solvent was removed at low pressure and the product was recrystallized from ethanol. Yield 51%; m.p. 53-54 °C; white solid; R_f = 0.74 (*n*-hexane:ethyl acetate; 7:3); IR (KBr) ν_{max}/cm^{-1} 2916, 2859, 1751, 1215, 1613, 918; ^{1}H NMR ($CDCl_3$, 300 MHz) δ 0.8 (t, 3H, *J* 6.9 Hz, CH_3), 1.2-1.5 (m, 12H, $(CH_2)_6$), 2.1 (m, 2H, CH_2CH_2N), 2.3 (s, 3H, CH_3), 4.6 (t, 2H, *J* 7.2 Hz, NCH_2), 6.9 (d, 2H, *J* 8.8 Hz, Ar–H), 8.0 (d, 2H, *J* 8.8 Hz, Ar–H); ^{13}C NMR ($CDCl_3$, 75 MHz) δ 14.1, 21.2, 22.6, 26.4, 28.9, 29.2, 29.3, 29.4, 31.8, 53.3, 122.2, 125.3, 128.1, 152.1, 164.3, 169.2.

(*ii*) 4-(2-Nonyl-2*H*-tetrazol-5-yl)phenol (**3**): The 4-(2-Nonyl-2*H*-tetrazol-5-yl)phenyl acetate (1.023 g, 3.1 mmol) was added to 20 mL methanol followed by addition of potassium hydroxide (1.17 g, 3.1 mmol) in 5 mL of water and refluxed for 12 h. The mixture was cooled to room temperature, filtered off and was concentrated on a rotary evaporator. The mixture was poured onto 100 g of ice and acidified with concentrated HCl to pH 2. The precipitated solid was filtered and purified by crystallization from ethanol. Yield 87%; white solid; m.p. 70 °C; R_f = 0.72 (*n*-hexane:ethyl acetate; 7:3); IR (KBr) ν_{max}/cm^{-1} 3163, 2924, 1613, 845; ^{1}H NMR ($CDCl_3$, 300 MHz) δ 0.9 (t, 3H, *J* 6.9 Hz, CH_3), 1.4-1.3 (m, 12H, $(CH_2)_6$), 2.1 (m, 2H, CH_2CH_2N), 4.6 (t, 2H, *J* 7.2 Hz, NCH_2), 6.9 (d, 2H, *J* 8.8 Hz, Ar–H), 8.0 (d, 2H, *J* 8.8 Hz, Ar–H); ^{13}C NMR ($CDCl_3$, 75 MHz) δ 14.1, 22.6, 26.4, 28.9, 29.2, 29.3, 29.4, 31.8, 53.2, 115.9, 119.7, 128.5, 157.9, 164.9.

4-Chlorobutyl acetate (**5**): To a solution of tetrahydrofuran (25.2 g, 0.35 mol) and zinc chloride (20 mg) at 0 °C was added dropwise acetyl chloride (23.5 g, 0.30 mol) and the solution was stirred for 40 min at this temperature followed by 30 min at room temperature and refluxed for 4 h more. The reaction mixture was dissolved in diethyl ether (200 mL) and the organic phase was washed with $NaHCO_3$ 5% (100 mL), water (100 mL), NaCl solution (100 mL) and again water (100 mL). The organic phase was dried over anhydrous sodium sulfate and distilled. Yield 71%; b.p. 95 °C at 24 mmHg (b.p. 92 °C at 22 mmHg)[24]; IR (KBr) ν_{max}/cm^{-1} 2960, 1735, 1340, 1250, 1070, 930, 725, 650; ^{1}H NMR ($CDCl_3$, 300 MHz) δ 1.6 (m, 4H, $(CH_2)_2$), 1.8 (s, 3H, CH_3), 3.4 (m, 2H, CH_2Cl), 3.9 (t, 2H, *J* 6.3 Hz, CH_2O).

4-[(4-Propenoyloxy)butyloxy]benzoic acid (**6**):[25] In a Dean-Stark apparatus were added 4-(ω-hydroxybutoxy) benzoic acid (7.7 g, 0.037 mol), acrylic acid (23.0 g, 0.324 mol) chloroform (150 mL), *p*TSA (1.5 g, 0.008 mol) and hydroquinone (1.5 g, 0.014 mol). The mixture was refluxed until the end of the reaction. After a standard workup procedure the product was recrystallized from isopropanol. Yield 65%; m.p. 120 °C; IR (KBr) ν_{max}/cm^{-1} 2940 (broad), 1750, 1680, 1580, 1260, 1080, 930; ^{1}H NMR ($CDCl_3$, 300 MHz) δ 1.8 (m, 4H, CH_2), 4.1 (m, 2H, CH_2O), 4.2 (s, 2H, CH_2O), 5.8 (dd, 1H, $^2J_{gem}$ 1.8 Hz, $^3J_{cis}$ 10.8 Hz, CH=CH_2), 6.1 (dd, 1H, $^3J_{cis}$ 10.2 Hz, $^3J_{trans}$ 17.1 Hz, CH=CH_2), 6.4 (dd, 1H, $^2J_{gem}$ 1.5 Hz, $^3J_{trans}$ 17.4 Hz, CH=CH_2), 6.8 (d, 2H, *J* 8.0 Hz, Ar–H), 8.0 (d, 2H, *J* 8.0 Hz, Ar–H).

4-[(4-Propenoyloxy)undecyloxy]benzoic acid (**8**): Compound **8** was synthesized according to reference 14 and Ritter *et al.*.[26] Yield 85%; white solid; m.p. 94 ºC; IR (KBr) ν_{max}/cm^{-1} 3080-2700, 2929, 2853, 1718, 1685, 1605, 1464, 1250, 1177, 1037, 854, 772; ^{1}H NMR ($CDCl_3$, 300 MHz) δ 1.3 (m, 14H, $(CH_2)_7$), 1.7 (m, 4H, $(CH_2)_2$), 4.1 (m, 4H, CH_2O), 5.8 (m, 1H, CH=CH_2), 6.1 (m, 1H, CH=CH_2), 6.4 (m, 1H, CH=CH_2), 6.9 (d, 2H, *J* 9.0 Hz, Ar–H), 8.0 (d, 2H, *J* 8.8 Hz, Ar–H).

Monomers **9** and **10**: General procedure. Acids **6** or **8** (0.005 mol), 4-(2-nonyl)-2*H*-tetrazol-5-ylphenol (**3**) (0.0055 mol), DCC (0.006 mol) and *p*TSA (0.0026 mol) were dissolved in freshly distilled pyridine (5 mL). The reaction was stirred for 3 days at room temperature. The mixture was filtered and washed with chloroform. The organic phase was washed with 10% cold aqueous hydrochloric acid (100 mL) and water and dried over sodium sulfate. The solvent was removed in a rotatory evaporator and the crude solid was purified by recrystallization from methanol.

4-(2-Nonyl-2*H*-tetrazol-5-yl)phenyl 4-[(propionyloxy) butyloxy)]benzoate (**9**): Yield 54%; white solid; m.p. 67-68 ºC; R_f = 0.74 (*n*-hexane: ethyl acetate; 7:3); IR (KBr) ν_{max}/cm^{-1} 2935, 2856, 1720, 1611, 1250, 765; ^{1}H NMR ($CDCl_3$, 300 MHz) δ 0.8 (t, 3H, *J* 6.0 Hz, CH_3), 1.3-2.5 (m, 18H, $(CH_2)_9$), 4.0-4.3 (m, 4H, CH_2O), 4.6 (t, 2H, *J* 7.2 Hz, CH_2N), 5.8 (dd, 1H, $^3J_{cis}$ 10.2 Hz, $^2J_{gem}$ 1.6 Hz, CH=CH_2), 6.1 (dd, 1H, $^3J_{cis}$ 10.2 Hz, $^3J_{trans}$ 17.3 Hz, CH=CH_2), 6.4 (dd, 1H, $^3J_{trans}$ 17.3 Hz, $^2J_{gem}$ 1.7 Hz, CH=CH_2), 6.9 (d, 2H, *J* 8.0 Hz, Ar–H), 7.3 (d, 2H, *J* 7.4 Hz, Ar–H), 8.0 (2H, d, *J* 8.0 Hz, Ar–H), 8.2 (d, 2H, *J* 7.3 Hz, Ar–H); ^{13}C NMR ($CDCl_3$, 75 MHz) δ 14.1, 14.2, 21.1-29.4, 31.8, 53.3, 60.4, 64.4, 67.6, 114.3, 121.6, 122.3, 125.2, 128.0, 132.4, 152.5, 163.6, 164.4, 164.5, 171.1.

4-(2-Nonyl-2*H*-tetrazol-5-yl) phenyl 4-[(propionyloxy) undecyloxy)]benzoate (**10**): Yield 35%; white solid; m.p. 73-75 °C; R_f = 0.74 (*n*-hexane: ethyl acetate; 7:3); IR (KBr) ν_{max}/cm^{-1} 2919, 2849, 2355, 1720, 1611, 1258, 765; ^{1}H NMR ($CDCl_3$, 300 MHz) δ 0.8 (t, 3H, *J* 6.9 Hz, CH_3), 1.3-2.0 (m, 32H, $(CH_2)_{16}$), 4.1 (t, 2H, *J* 6.5 Hz, CH_2O), 4,15 (t, 2H, *J* 6.8 Hz, CH_2O), 4.6 (t, 2H, *J* 7.2 Hz, CH_2N), 5.8 (dd, 1H, $^2J_{gem}$ 1.5 Hz, $^3J_{cis}$ 10.4 Hz, CH=CH_2), 6.1 (dd, 1H, $^3J_{cis}$ 10.4 Hz, $^3J_{trans}$ 17.3 Hz, CH=CH_2), 6.4 (dd, 1H, $^2J_{gem}$ 1.5 Hz, $^3J_{cis}$ 17.3 Hz, CH=CH_2), 6.9 (d, 2H, *J* 9.0 Hz, Ar–H), 7.3 (d, 2H, *J* 8.8 Hz, Ar–H), 8.1 (d, 2H, *J* 8.9 Hz, Ar–H), 8.2 (d, 2H, *J* 8.8 Hz, Ar–H); ^{13}C NMR ($CDCl_3$, 75 MHz) δ 14.0, 14.2, 29.6-21.0, 31.8, 53.2, 60.3, 64.5, 68.3, 114.3, 121.3, 122.3, 125.1, 128.0, 132.3, 152.6, 163.6, 164.4, 164.6, 171.1.

Polymerization reaction: In a Schlenk flask dry toluene was added under inert atmosphere followed by addition of 0.001 mol of the monomer (**9** or **10**). The mixture was stirred for 30 min at room temperature. To this mixture AIBN (3 or 5 wt.%) was added and the reaction mixture was further heated at 70 ºC for 72 h. After completion of the reaction the mixture was poured into cold methanol to precipitate the product. The solid was filtered and washed several times with ethyl acetate to separate the unreacted monomer, which left behind pure polymers **11a**,**b** and **12**.

Poly-{4-(2-nonyl-2H-tetrazol-5-yl)phenyl 4-[(propionyloxy)butyloxy)]}benzoate (**11a,b**): Yields 69% for **11a** and 85% for **11b**; white solid; IR (neat) ν_{max}/cm^{-1} 2935, 2856, 1720, 1611, 1250, 765; ^{1}H NMR ($CDCl_3$, 300 MHz) δ 0.9 (m, 3H, CH_3), 1.2-2.0 (m, 18H, m), 4.0-4.2 (m, 4H, CH_2O), 4.6 (m, 2H, CH_2N), 6.9 (m, 2H, Ar–H), 7.3 (m, 2H, Ar–H), 8.1 (m, 2H, Ar–H), 8.2 (m, 2H, Ar–H); ^{13}C NMR ($CDCl_3$, 75 MHz) δ 14.2, 21.1-29.4, 31.8, 53.3, 64.4, 67.6, 114.3, 121.6, 122.3, 125.2, 128.0, 132.4, 152.5, 163.6, 164.4, 164.5, 171.1.

Poly-{4-(2-nonyl-2H-tetrazol-5-yl)phenyl 4-[(propionyloxy) undecyloxy)]}benzoate (**12**): Yield 78%; white solid; IR (neat) ν_{max}/cm^{-1} 2919, 2849, 2355, 1720, 1611, 1258, 765; ^{1}H NMR ($CDCl_3$, 300 MHz) δ 0.8 (t, 3H, *J* 6.9 Hz, CH_3), 1.2-2.0 (m, 32H), 4.0-4.1 (m, 4H), 4.6 (m, 2H, CH_2O), 6.9 (m, 2H, Ar–H), 7.3 (m, 2H, Ar–H), 8.1 (m, 2H, Ar–H), 8.2 (m, 2H, Ar–H); ^{13}C NMR ($CDCl_3$, 75 MHz) δ 14.2, 21.1-29.4, 31.8, 31.8, 53.2, 64.5, 68.3, 114.3, 121.3, 122.3, 125.1, 128.0, 132.3, 152.6, 163.6, 164.4, 164.6, 171.1.

Supplementary Information

Supplementary data (^{1}H and ^{13}C NMR spectra) are available free of charge at http://jbcs.sbq.org.br as PDF file.

Acknowledgements

The authors gratefully acknowledge INCT-Catalise, Fapergs-Edital PqG 2012, Edital 01/12-PPG-Química-UFRGS and thank LDRX-DF/UFSC for the X-ray diffraction experiments. We also thank the Higher Education Commission of Pakistan for their support. M. Tariq thanks TWAS-CNPq program for financial assistance for accomplishing this valuable work.

References

1. Chien, L.-C.; Lin, C.; Fredley, D.; MacCargar, J.; *Macromolecules* **1992**, *25*, 133.
2. Ringsdorf, H.; Schmidt, H.-W.; Schneller, A.; *Makromol. Chem., Rapid Commun*. **1982**, *3*, 745.
3. Mori, A.; Hirayama, R.; Kato, N.; Takeshita, H.; Ujiu, S.; *Chem. Lett.* **1997**, *26*, 509.
4. Mikami, K.; Yajima, T.; Terada, M.; Kawauchi, S.; Suzuki, Y.; Kobayashi, I.*; Chem. Lett.* **1996**, *25*, 861.
5. Kusumoto, T.; Ogino, K.; Hiyama, T.; Isozaki, T.; Suzuki, Y.; *Chem. Lett.* **1996**, *26*, 865.

6. Tashiro, K.; Hou, J.-A.; Kobayashi, M.; Inoue, T.; *J. Am. Chem. Soc*. **1990**, *112*, 8273.
7. Passo, J. A.; Merlo, A. A.; Eccher, J.; Bechtold, I. H.; Kelly, S. M.; *Quim. Nova* **2012**, *35*, 1527; Rao, B. V. V. S. N. P.; Mathur, S. C.; Dube, D. C.; Tewari, D. P.; Banerjee, M.; *Can. J. Chem*. **1997**, *75*, 1041.
8. Chang, J. Y.; Baik, J. H.; Lee, C. B.; Han, M. J.; Hong, S.-K.; *J. Am. Chem. Soc*. **1997**, *119*, 3197.
9. Wang, J.-W.; Zhang, B.-Y.; *J. Mater. Sci.* **2014***, 49,* 604.
10. da Silva, L.; Gallardo, H.; Magnago, R. F.; Begnini, I. M.; *Mol. Cryst. Liq. Cryst*. **2005**, *432*, 1.
11. Gallardo, H.; Magnago, R. F.; Bortoluzzi, A.; *Liq. Cryst.* **2001**, *28*, 1343.
12. dos Santos, D. R.; de Oliveira, A. G. S.; Coelho, R. L.; Begnini, I. M.; Magnago, R. F.; da Silva, L.; *ARKIVOC* **2008**, *xvii*, 157.
13. Merlo, A. A.; Tariq, M.; Hameed, S.; Bechtold, I. H.; Bortoluzzi, A. J.; *J. Mater. Chem. C* **2013**, *1*, 5583.
14. Holmberg, K.; Hansen, B.; *Acta Chem. Scand., Ser. B* **1979**, *33*, 410.
15. Portugal, M.; Ringsdorf, H.; Zentel, R.; *Makromol. Chem*. **1982**, *183*, 2311; Whitcombe, M. J.; Davis, F. J.; Gilbert, A.; Mitchell, G. R.; *Polym. Commun*. **1991**, *32*, 380.
16. Gray, G. W.; Goodby, J. W. G.; *Smectic Liquid Crystals: Textures and Structures;* Leonard Hill: Glasgow, 1984.
17. Ritter, O. M. S.; Merlo, A. A.; Pereira, F. V.; da Silveira, N. P.; Geissler, E.; Zukerman-Schpector, J.; *Liq. Cryst.* **2002**, *29*, 1187.
18. Wang, X.-J.; Zhou, Q.-F.; *Liquid Crystalline Polymers*; World Scientific Publishing Co. Pte. Ltd: Singapore, 2004, ch. 3.
19. Tsukruk, V. V.; Shilov, V. V.; *Polymer* **1990**, *31*, 1793.
20. Craig, A. A.; Imrie, C. T.; *Macromolecules* **1999**, *32*, 6215.
21. Imrie, C. T.; Schleeh, T.; Karasz, F. E.; Attard, G. S.; *Macromolecules* **1993**, *26*, 539.
22. Boeffel, C; Spiess, H. W. In *Side Chain Liquid Crystal Polymers*; McArdle, C. B., ed.; Blackie & Son: New York, 1989, ch. 7-8.
23. Passo, J. P.; Vilela, G. D.; Schneider, P. H.; Ritter, O. M. S.; Merlo, A. A.; *Liq. Cryst*. **2008**, *35*, 833; Ritter, O. M. S.; Giacomelli, F. C.; Passo, J. A.; da Silveira, N. P.; Merlo, A. A.; *Polym. Bull.* **2006**, *56*, 549.
24. Pasha, M. A.; Manjula, K.; *Synth. Commun.* **2011**, *41*, 2309.
25. Pereira, F.; Pesce, N. S.; Magnago, R. V.; Vollmer, A. F.; Mauler, R. S.; Merlo, A. A.; *Polym. Bull.* **1999**, *42*, 551.
26. Ritter, O. M. S.; Pereira, F. V.; Vieira, C. H.; da Silveira, N. P.; Merlo, A. A.; *J. Braz. Chem. Soc.* **2001**, *12*, 184.

Submitted: March 27, 2014
Published online: May 20, 2014

J. Braz. Chem. Soc., Vol. 25, No. 7, S1-S6, 2014.
Printed in Brazil - ©2014 Sociedade Brasileira de Química
0103 - 5053 $6.00+0.00

Supplementary Information

Side-Chain Liquid-Crystalline Polymer Tetrazoles: Synthesis and Characterization

Muhammad Tariq,[a,b] Shahid Hameed,*[,b] Rachel F. Magnago,[c] Ivan H. Bechtold[d] and Aloir A. Merlo*[,a]

[a]Instituto de Química, Universidade Federal do Rio Grande do Sul (UFRGS), Av. Bento Gonçalves, 9500, Bairro Agronomia, 91501-970 Porto Alegre-RS, Brazil

[b]Department of Chemistry, Quaid-i-Azam University, 45320 Islamabad, Pakistan

[c]Unidade Tecnológica, Universidade do Sul de Santa Catarina (Unisul), Av. Pedra Branca, 25, Cidade Universitária, 88137-270 Palhoça-SC, Brazil

[d]Departamento de Física, Universidade Federal de Santa Catarina (UFSC), Bairro Trindade, 88040-900 Florianópolis-SC, Brazil

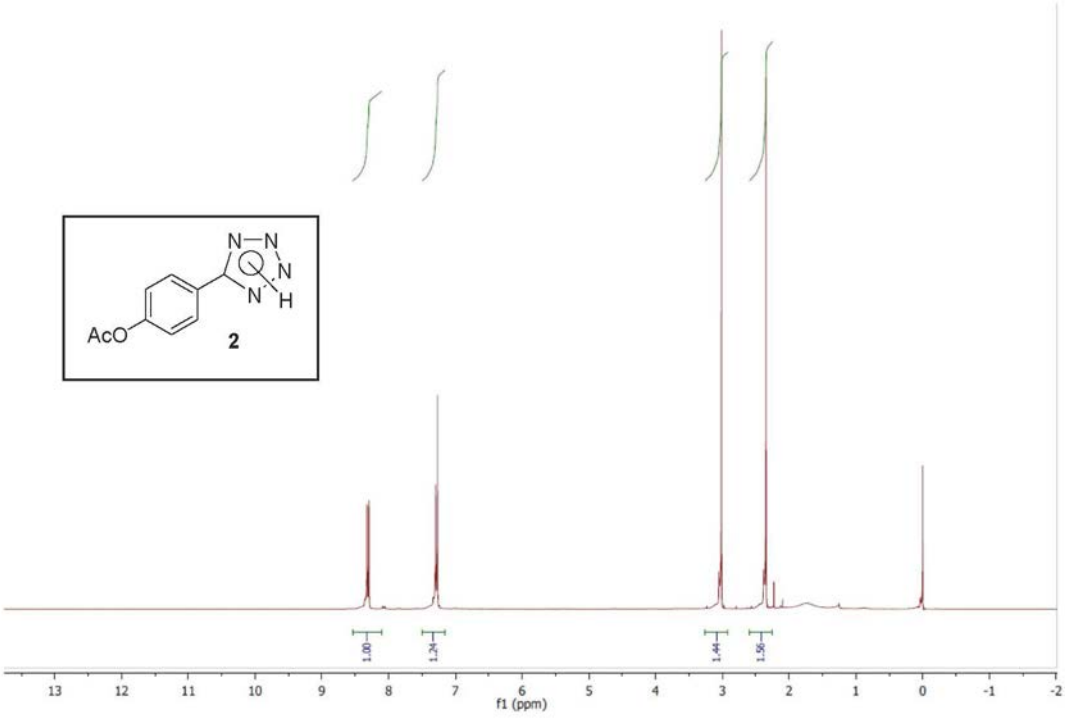

Figure S1. ^{1}H NMR spectrum ($CDCl_3$, 300 MHz) of **2**.

*e-mail: aloir.merlo@ufrgs.br

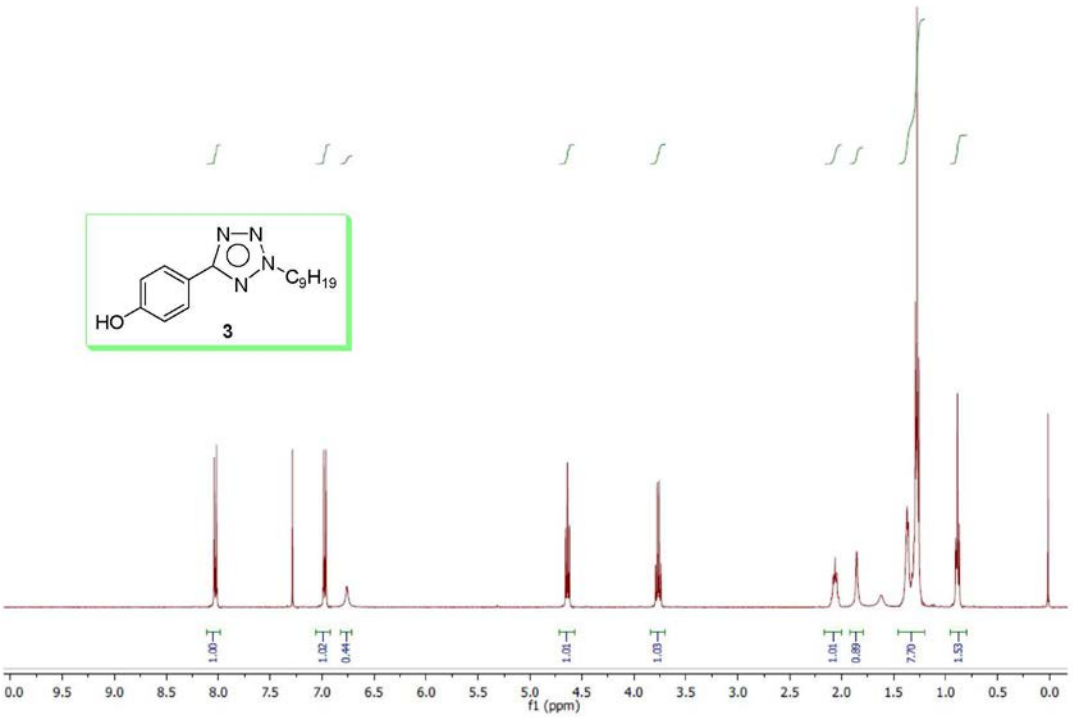

Figure S2. ^{1}H NMR spectrum ($CDCl_3$, 300 MHz) of **3** (solvent peak at 3.7 ppm).

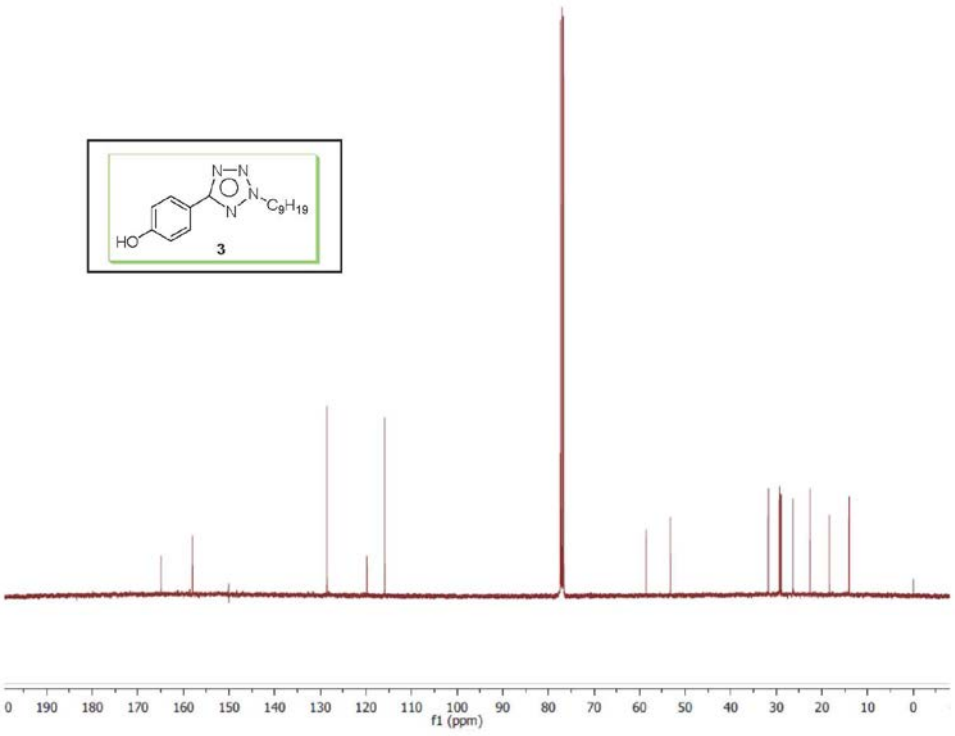

Figure S3. ^{13}C NMR spectrum ($CDCl_3$, 75 MHz) of **3**.

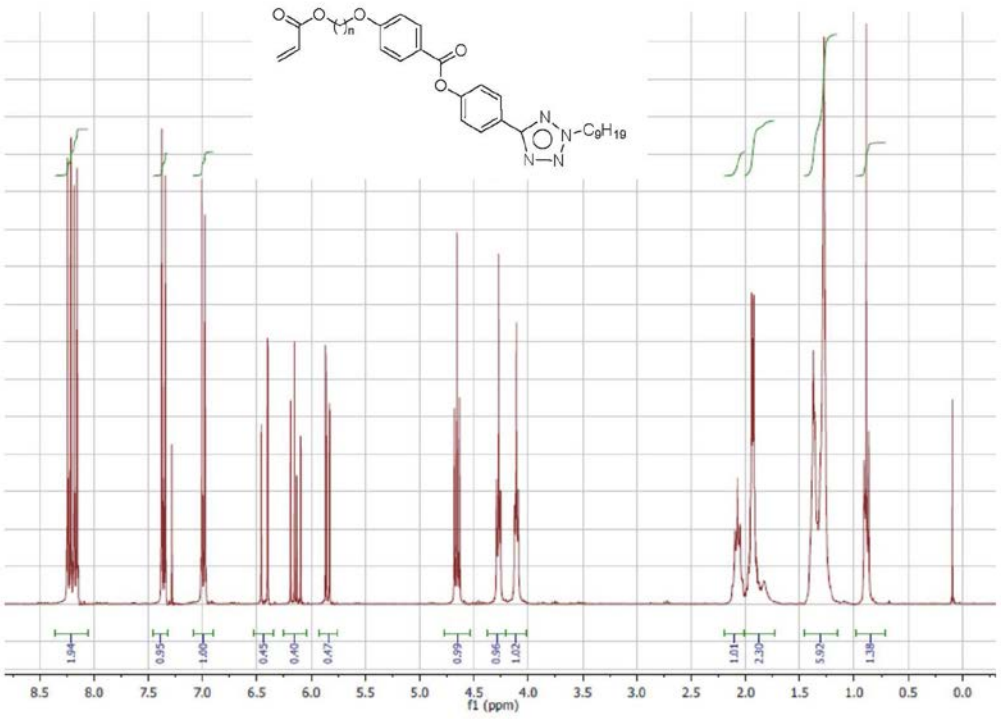

Figure S4. ^{1}H NMR spectrum ($CDCl_3$, 300 MHz) of monomer **9** (n = 4).

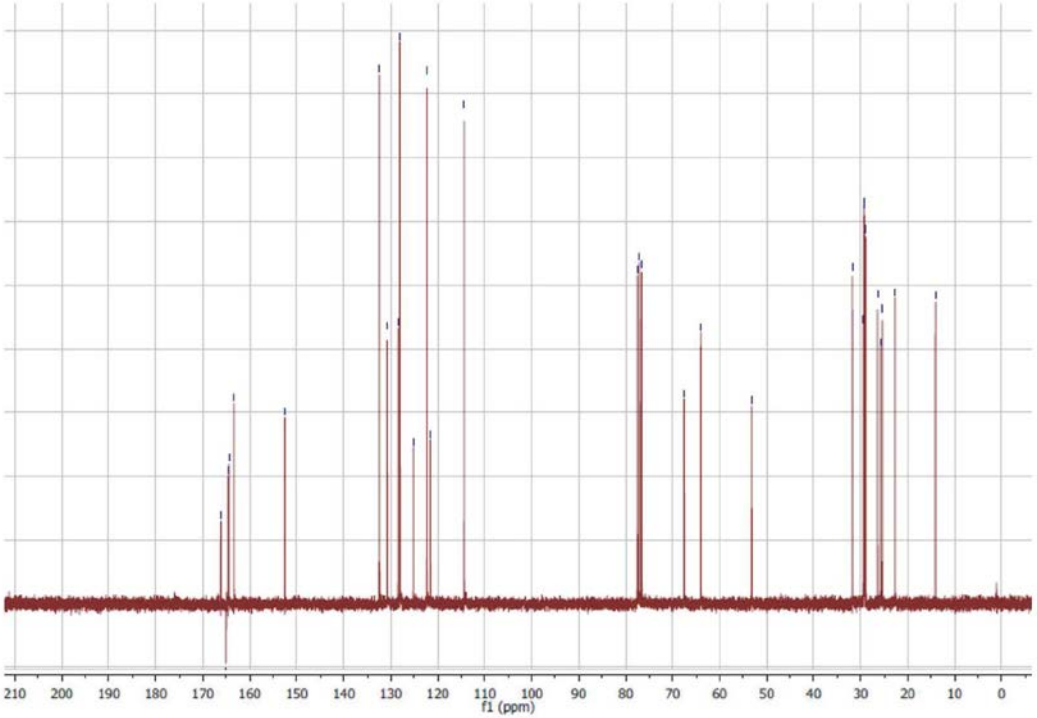

Figure S5. ^{13}C NMR spectrum ($CDCl_3$, 75 MHz) of monomer **9** (n = 4).

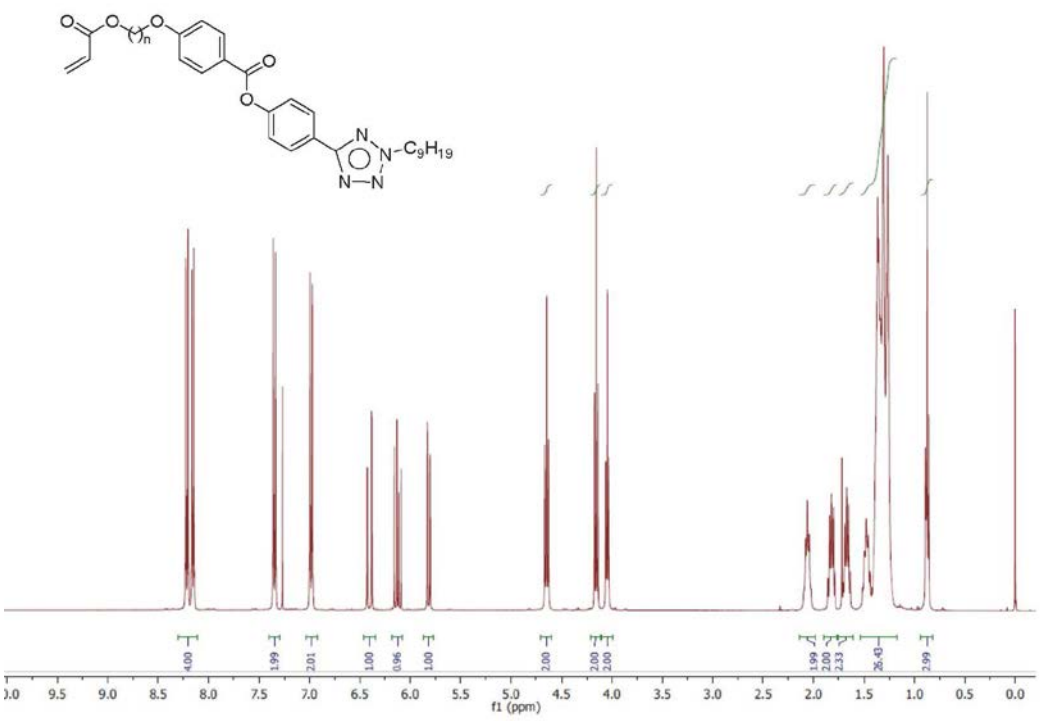

Figure S6. ^{1}H NMR spectrum ($CDCl_3$, 300 MHz) of monomer **10** (n = 11).

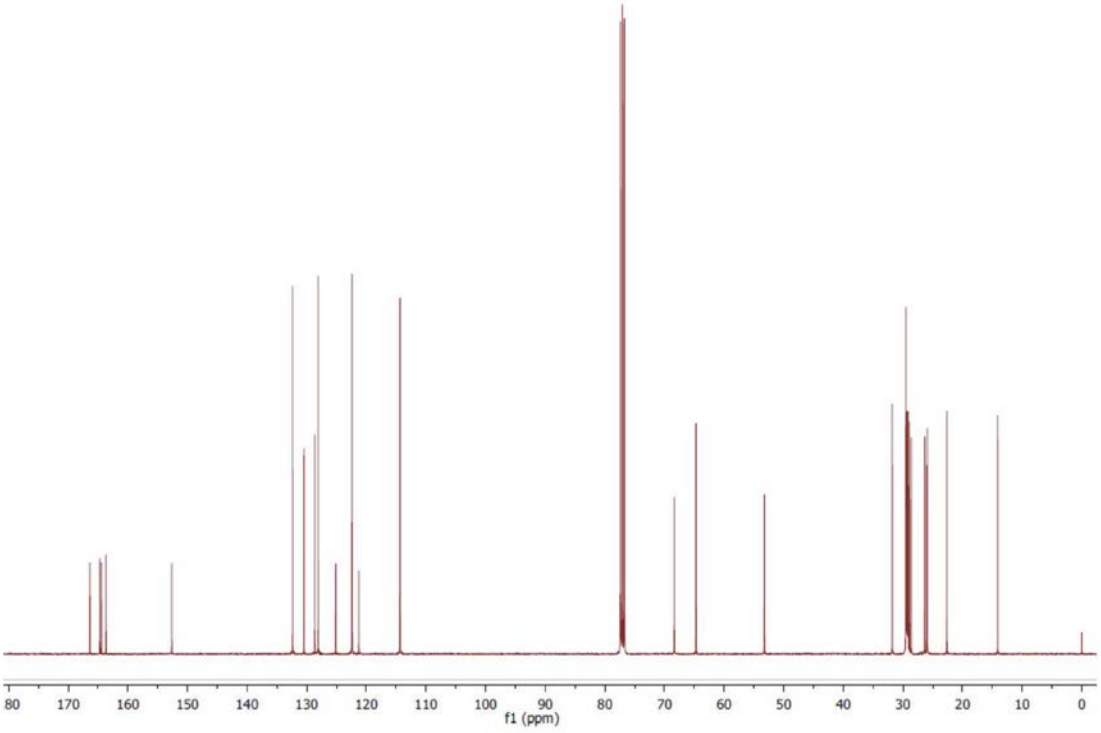

Figure S7. ^{13}C NMR spectrum ($CDCl_3$, 75 MHz) of monomer **10** (n = 11).

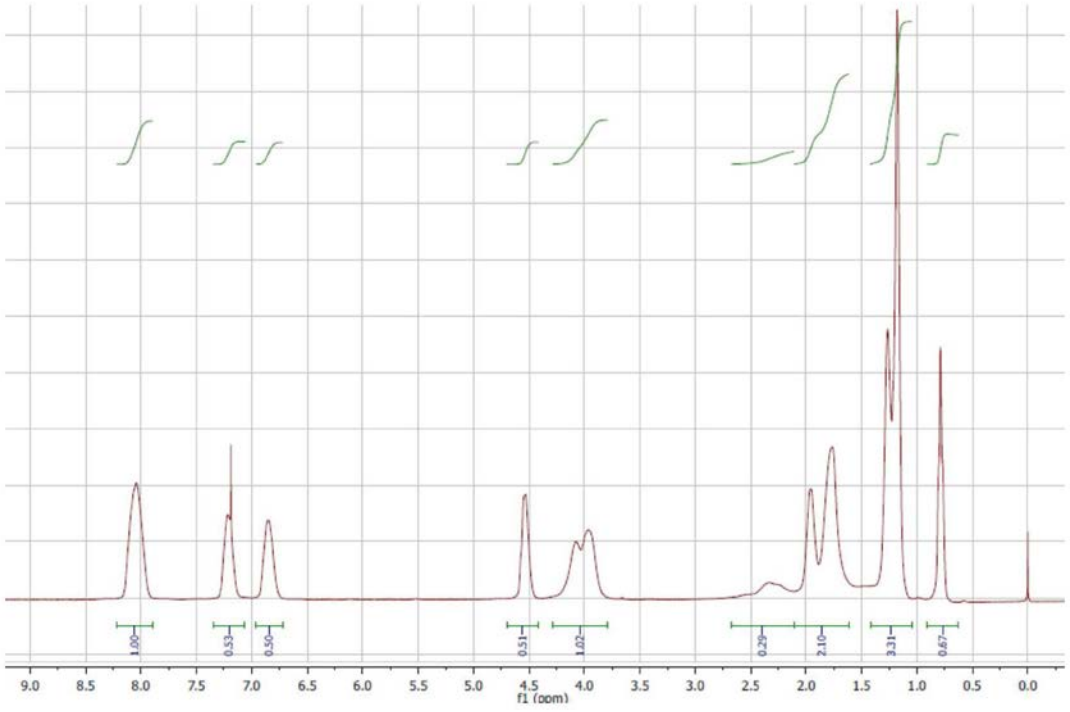

Figure S8. ^{1}H NMR spectrum ($CDCl_3$, 300 MHz) of polymer **11a** (n = 4).

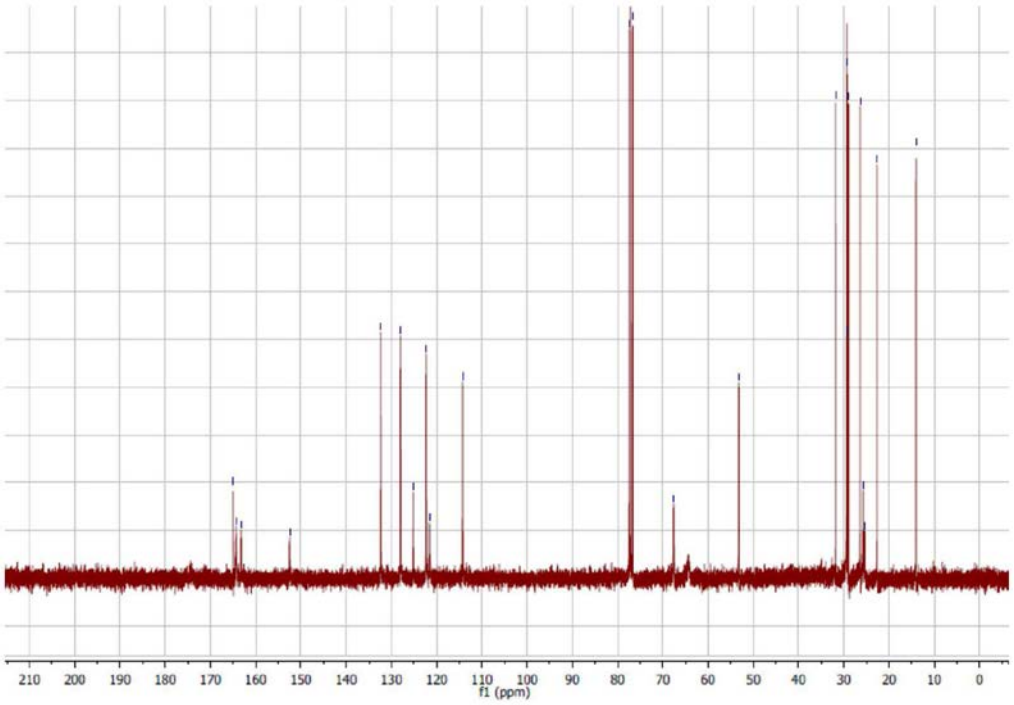

Figure S9. ^{13}C NMR spectrum ($CDCl_3$, 75 MHz) of polymer **11a** (n = 4).

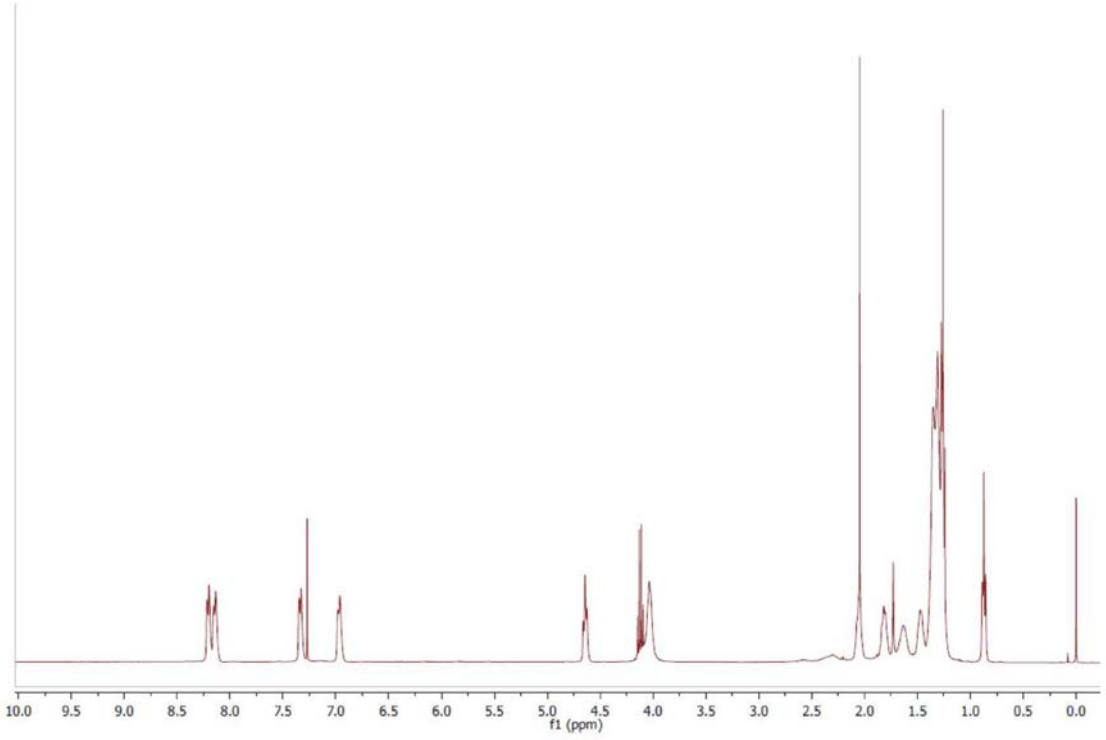

Figure S10. ^{1}H NMR spectrum ($CDCl_3$, 300 MHz) of polymer **12** (n = 11).